Quantum modeling of thermoelectric performance of strained Si/Ge/Si superlattices using the nonequilibrium Green's function method

A. Bulusu
Interdisciplinary Materials Science, Vanderbilt University, Nashville, Tennessee 37235, USA

D. G. Walker[a)]
Department of Mechanical Engineering, Vanderbilt University, Nashville, Tennessee 37235, USA

(Received 9 July 2007; accepted 14 August 2007; published online 11 October 2007)

The cross-plane thermoelectric performance of strained Si/Ge/Si superlattices is studied from a quantum point of view using the nonequilibrium Green's function method. Strain causes the germanium well layers to turn into barriers that promote electron tunneling through the barriers. Electron tunneling produces oscillations in the Seebeck coefficient due to shift in subband energies near the Fermi level. Strain-induced energy splitting can increase the power factor by up to four orders of magnitude in germanium-rich substrates. Also, at large doping, strain lowers the subband energies such that thermoelectric performance is independent of layer thickness between 2 and 4 nm germanium barrier layers. The results imply that larger barrier layers can be used at high doping without a performance penalty while avoiding problems with interlayer diffusion that are prevalent in films with small thicknesses. © *2007 American Institute of Physics*. [DOI: 10.1063/1.2787162]

I. INTRODUCTION

Substrate strain has a dramatic influence on the electrical properties of silicon films. For example, metal-oxide-semiconductor field-effect transistors (MOSFETs) in the presence of strain have been designed with remarkable improvements in their performance. Consequently, strain in microelectronic devices has been studied extensively.[1–4] Strain effects on the electrical performance of thermoelectric devices have also been studied from a phenomenological point of view.[5] However, a quantum treatment of transport in superlattice structures in the presence of strain is lacking. Quantum effects are important in these structures because strain ultimately alters the band structure, which promotes or restricts tunneling between layers. In this work, we explore the effect of lattice strain on the thermoelectric properties of superlattice structures from a quantum point of view.

Strain splits the sixfold degenerate conduction bands in silicon into twofold and fourfold degenerate bands with the energy of the twofold degenerate bands being lower than that of the fourfold degenerate bands. For example, when a silicon (001) layer is under tensile strain, the conduction band minima along the [100] and [010] axes are raised in energy while the band minima along the [001] axis is lowered. Electrons tend to occupy the bands with lower energy, i.e., along the [001] direction, which have lower effective mass in the plane of the axis. The lower effective mass along the in-plane directions ensures higher electron mobility in the plane of the (001) layers. The improvement in mobility along with the decrease in intervalley scattering between the twofold and fourfold valleys has been exploited to produce MOSFETs with higher electrical conductivity.[6]

Quantum well superlattices have gained attention in the past decade as thermoelectric materials due to a number of advantages. (1) The Seebeck coefficient S can be improved by the increase in the local density of states per unit volume near the Fermi energy,[5] and (2) the thermal conductivity κ can be decreased due to phonon confinement[7,8] and phonon scattering at the material interfaces in the superlattice.[5,9–11] Si/Ge superlattices are commonly grown on buffer layers consisting of a fixed concentration of Si_xGe_{1-x} alloy on which alternate layers of silicon and germanium are epitaxially grown.[5,12] In the case of a heterojunction superlattice, strain has a contrasting influence on the superlattice layers. For example, in the case of a Si(001)/Ge(001) superlattice grown on a Si_xGe_{1-x} substrate, the conduction band minima along the silicon [001] direction is lowered in energy while the conduction band minima along the [001] direction in the germanium layers is increased in energy. As a result, the germanium layers in the cross-plane direction confine electrons to the silicon layers due to their higher conduction band edges. In addition to electron confinement due to germanium barrier layers, reduced dimensionality in the superlattice layers also leads to electron confinement, resulting in the formation of subbands. If the germanium barrier layers are sufficiently thin, electrons can tunnel through the germanium layers which will significantly affect the electrical performance of the superlattice.

Incorporating the effect of substrate strain on the thermoelectric performance of superlattices requires a quantum transport model that can successfully incorporate wave effects such as electron tunneling and diffraction to predict thermoelectric performance. Models based on Boltzmann and Fermi-Dirac statistics coupled in semiclassical transport have been very effective in identifying the pertinent physical parameters responsible for thermoelectric performance in bulk materials. However, wave effects found in nanostructured materials cannot be captured naturally in such particle-based models without introducing some kind of correction

[a)]Author to whom correspondence should be addressed. Electronic mail: greg.walker@vanderbilt.edu

terms.[13] A quantum transport model to calculate thermoelectric performance of strained superlattices is introduced through the nonequilibrium Green's function (NEGF) method. The NEGF method does not require a statistical distribution of carriers. This allows for the modeling of highly nonequilibrium transport. A description of the NEGF model is given in Ref. 14 while its application to modeling the thermoelectric performance of nanostructures can be found in Refs. 15 and 16.

The NEGF method uses an effective mass Hamiltonian H to solve the Schrödinger wave equation as shown in Eq. (1). U is the channel potential and ε_α corresponds to the energy eigenvalues of the channel. Current flow from the contacts is modeled as a modification of the channel density of states through self-energy terms in the Hamiltonian,

$$(H+U)\psi_\alpha(\mathbf{r}) = \varepsilon_\alpha(\mathbf{r}). \tag{1}$$

The effective mass Hamiltonian for the superlattice is calculated using the finite difference method where the conduction band edges in silicon, germanium, and the interface are included as shown by

$$[H] = \begin{bmatrix} E_{c_{\mathrm{Si}}} + 2t_{\mathrm{Si}} & -t_{\mathrm{Si}} & 0 \\ -t_{\mathrm{Si}} & E_{c_J} + t_{\mathrm{Si}} + t_{\mathrm{Ge}} & -t_{\mathrm{Ge}} \\ 0 & -t_{\mathrm{Ge}} & E_{c_{\mathrm{Ge}}} + 2t_{\mathrm{Ge}} \end{bmatrix}. \tag{2}$$

Here, t is the interunit coupling energy and is written as a function of the effective mass m^* and the grid spacing a as

$$t = \frac{\hbar^2}{2m^* a^2}. \tag{3}$$

Van de Walle[17] in 1989 developed a theory to calculate the change in the band structure of materials under biaxial strain. According to his research, the shift in the conduction band with respect to its average value is given by

$$\Delta E_c^{001} = \tfrac{2}{3}\Xi_u^{\Delta}(\varepsilon_{zz} - \varepsilon_{xx}). \tag{4}$$

The strain tensors ε_{zz} and ε_{xx} are obtained from the difference in the in-plane and cross-plane lattice constants. Ξ_u is the hydrostatic deformation potential for the conduction band. Using Van de Walle's model, the change in the conduction band edges for silicon and germanium due to substrate strain are calculated for Si_xGe_{1-x} substrates with varying concentrations of silicon and germanium. The resulting band diagrams depicting the splitting of the conduction band edge along the Δ valley in silicon and germanium due to Si(001) and $Si_{0.5}Ge_{0.5}$, respectively, are shown in Fig. 1. The shift in the conduction band edges are incorporated into the NEGF model through the value of E_c in the Hamiltonian to obtain the current-voltage characteristics and the thermoelectric coefficients of strained Si/Ge/Si quantum well superlattice structures.

II. THERMOELECTRIC PROPERTIES OF STRAINED SI/GE/SI QUANTUM WELL SUPERLATTICE

Cross-plane Seebeck coefficient and electrical conductivity of Si/Ge/Si quantum well superlattices are studied using the NEGF model with the inclusion of substrate strain.

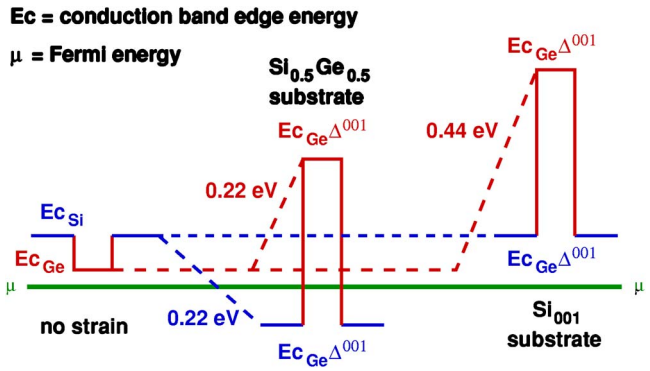

FIG. 1. (Color online) Change in band structure of silicon and germanium with strain for Si(001) and $Si_{0.5}Ge_{0.5}$ substrates.

The superlattice studied in this research consists of a single quantum well formed by alternating layers of silicon, germanium, and silicon thin films, as shown in Fig. 2. Electron confinement in the device occurs due to two reasons. (1) The very small thickness of the films gives rise to discretely spaced energy subbands in the cross-plane z direction. (2) The difference in the conduction band edges of the different materials forming the layers of the superlattice set up potential barriers to electron flow, thus causing additional confinement of the electrons in the well region. Electron transport in the device under an applied bias is modeled along the confined z direction and the current is calculated over the conduction band and ten subbands. The thickness of the films considered in this paper is less than the de Broglie wavelength of electrons at room temperature, allowing us to treat transport as ballistic in nature. Doping for each film in the superlattice is applied by changing the relative energy between the Fermi level and the conduction band edge for each material using the relation[18]

$$n = N_c \exp\left(-\frac{(E_c - E_f)}{k_B T}\right). \tag{5}$$

Figure 3 shows the calculated Seebeck coefficient of Si(2 nm)/Ge(2 nm)/Si(2 nm) superlattice structure grown on various Si_xGe_{1-x} substrates where x varies from 0 to 0.75. The Seebeck coefficient is also compared to measured values

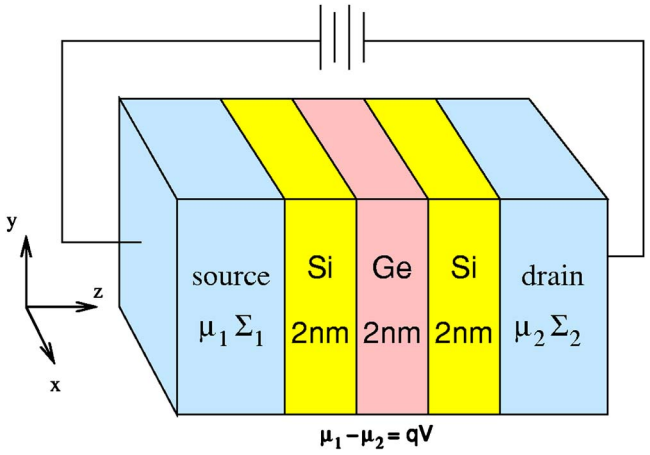

FIG. 2. (Color online) Schematic representation of a Si/Ge/Si quantum well superlattice modeled in the simulation.

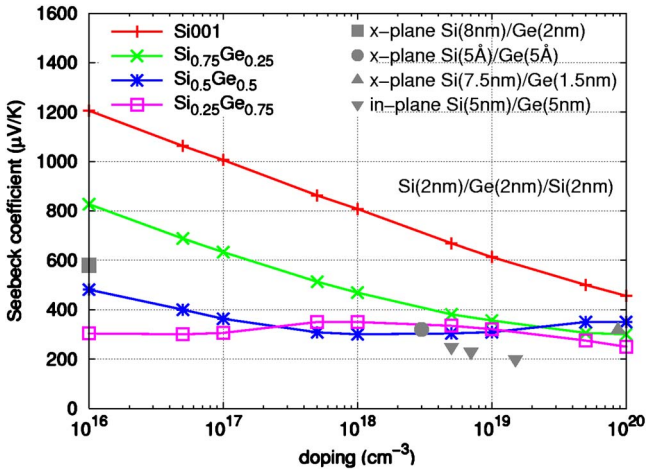

FIG. 3. (Color online) Seebeck coefficient vs doping for Si(2 nm)/Ge(2 nm)/Si(2 nm) superlattice for various substrates compared with experimental measurements (Refs. 12 and 19–22).

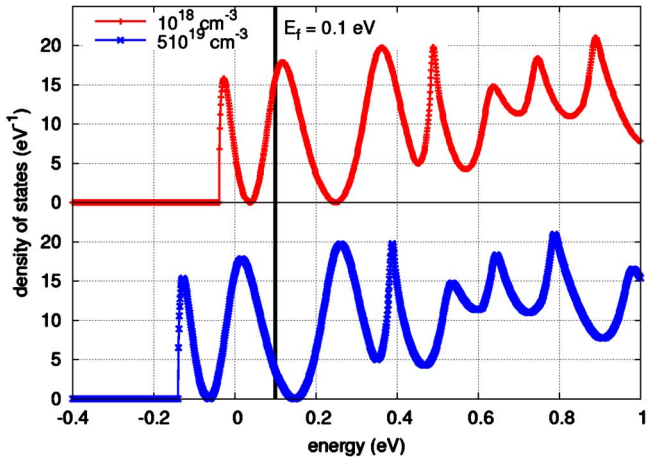

FIG. 5. (Color online) (a) Available density of states vs energy for 1×10^{18} cm^{-3} doping of the superlattice. (b) Density of states vs energy for 5×10^{18} cm^{-3} doping of superlattice. The red line in each case is the Fermi level.

from Refs. 12 and 19–22. Two important effects can be seen in Fig. 3. (1) Seebeck coefficient values of superlattice that is grown on plain Si(001) substrate are significantly larger than those of other substrates. (2) The Seebeck coefficient oscillates with doping in the case of the $Si_{0.5}Ge_{0.5}$ and $Si_{0.25}Ge_{0.75}$ substrates.

The reason for the higher Seebeck coefficient values for the Si(001) substrate can be explained by comparing the band diagrams of Si(2 nm)/Ge(2 nm)/Si(2 nm) superlattices that are grown on Si(001) substrate and $Si_{0.5}Ge_{0.5}$ substrates. Figure 4 shows the band diagrams of the Si(2 nm)/Ge(2 nm)/Si(2 nm) superlattice for a doping of 10^{18} cm^{-3} with respect to a reference Fermi level of 0.1 eV. As seen in Fig. 4, the conduction band edge in silicon does not change for a Si(001) substrate and is located at 0.0863 eV above the Fermi energy which is approximately equal to $3k_BT$ above the Fermi level. The germanium layer which experiences tensile strain along the [001] direction due to Poisson's stresses undergoes band splitting, causing its conduction band minima to increase in energy and form a significant barrier to the flow of electrons. For thermoelectric purposes when the temperature at the superlattice drain is increased, the electrons at the conduction band edge in silicon cannot easily diffuse nor drift through the superlattice due to the large germanium barrier, resulting in a large Seebeck voltage. In the case of a $Si_{0.5}Ge_{0.5}$ substrate, band splitting due to compressive stresses along the z axis in the silicon layer shifts its conduction band minima below the Fermi level. When the drain temperature is increased, electrons below the Fermi level gain energy and occupy the states immediately above the Fermi level on the drain side. The empty states below the Fermi level on the drain side attract electrons from the source that can tunnel through the germanium layer easily. The ability of electrons to tunnel through germanium means that the electron diffusion due to temperature is easily balanced by electron drift at low voltages. Hence, the Seebeck voltage developed is lower than that of the Si(001) substrate, leading to lower Seebeck coefficients.

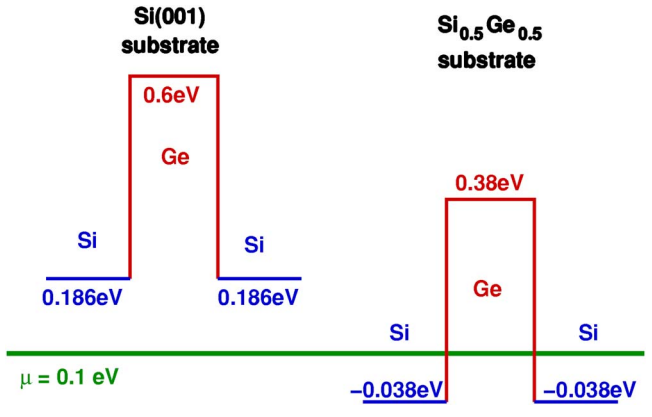

FIG. 4. (Color online) Band diagram of quantum well for a doping of 1×10^{18} cm^{-3} for Si(001) and $Si_{0.5}Ge_{0.5}$ substrates.

The oscillations in the Seebeck coefficient with doping for the $Si_{0.5}Ge_{0.5}$ and $Si_{0.25}Ge_{0.75}$ substrates can be explained by looking at the available density of states/eV distribution in the superlattice for the $Si_{0.5}Ge_{0.5}$ substrate shown in Fig. 5. It can be seen from Fig. 5(a) that for a few k_BT below the Fermi level, the density of states for the 10^{18} cm^{-3} doping case is approximately 12 states/eV and is higher than that of the 5×10^{19} cm^{-3} doping case in Fig. 5(b), which contains about 5 states/eV. When the drain temperature is raised, electrons from states below the Fermi level rise to states above it. However, with the limited availability of states below the Fermi level in the 5×10^{19} cm^{-3} doping case, the probability of electrons tunneling from the source side of the silicon layer is lower in the case of the 5×10^{19} cm^{-3}. As a result, more electrons can tunnel in the 10^{18} cm^{-3} doping case, resulting in a Seebeck coefficient that is smaller by 17% compared to the 5×10^{19} cm^{-3} doping case. It is evident from the results in Figs. 4 and 5 that, lower concentrations of silicon in the substrate alloy layer will result in greater strain in the silicon layer lowering its conduction band edge further below the Fermi level. The lower conduction band shifts the subbands closer to the Fermi level, leading to Seebeck oscillations, as seen from Fig. 4, where the $Si_{0.25}Ge_{0.75}$ substrate also displays oscillations in the Seebeck coefficient with

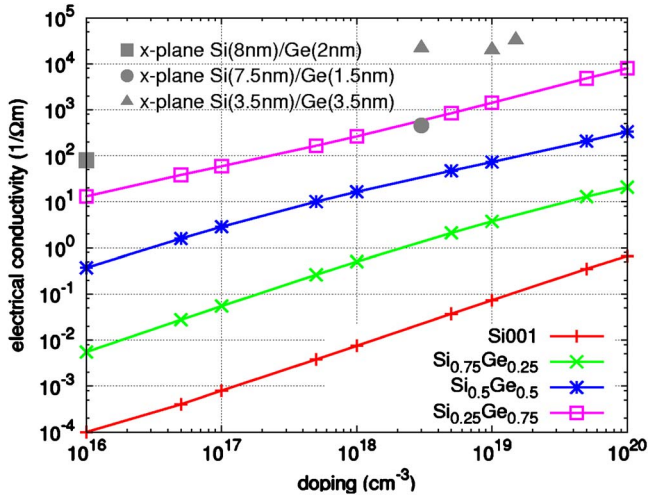

FIG. 6. (Color online) Electrical conductivity vs doping for Si(2 nm)/Ge(2 nm)/Si(2 nm) superlattice for various substrates compared with experimentally measured values (Refs. 12, 19, and 24).

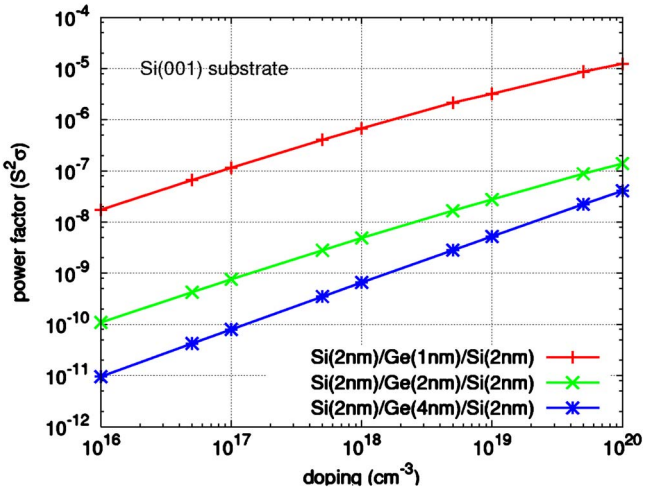

FIG. 8. (Color online) Power factor of various Si/Ge/Si superlattices with Si(001) substrate for varying thickness of germanium layer.

doping. This effect is only possible where confinement creates discrete density of states. Experimental evidence of increase in Seebeck coefficient with doping was reported by Vashaee *et al.*[23] In this case, the superlattice structure was made of 25 periods of InGaAs (5 nm)/InAlAs(3 nm) layers. The measured Seebeck coefficient was found to decrease with doping from 2×10^{18} to 8×10^{18} cm^{-3} after which it almost doubles for a doping of 3×10^{19} cm^{-3}. No sign change in the Seebeck coefficient was observed experimentally, indicating that transport was due to electrons and not holes.

Figure 6 shows the calculated electrical conductivity σ of the quantum well superlattice for various substrates as a function of doping. The conductivity for a given doping increases as the concentration of silicon in the substrate is reduced. The reason for this behavior is due to the fact that when the percentage of silicon in the substrate is reduced, the silicon layer is increasingly under in-plane tensile stress. As a result, the conduction band edge along the [001] direction in silicon is lowered relative to the Fermi level. Even though the value of $\Delta E_{c\text{Si–Ge}}$ does not change, the lowering of the silicon band edge with increase in the concentration of germanium in the substrate means that the germanium layer band energies will also be drawn closer to the Fermi level, opening more states for electron transport and hence better conductivity.

The dominance of the electrical conductivity on the power factor ($S^2\sigma$) is evident from Fig. 7 where despite the very high Seebeck coefficients of the superlattice grown on Si(001) substrate, the superlattice grown on $Si_{0.25}Ge_{0.75}$ substrate has the best power factor values due to its higher electrical conductivity compared to other substrates.

The usefulness of the NEGF method as a tool for designing and optimization of quantum well structures for enhanced thermoelectric performance is demonstrated through Figs. 8 and 9 where the power factor of Si/Ge/Si superlattices grown on Si(001) substrate and $Si_{0.5}Ge_{0.5}$ substrate is compared for three different germanium barrier layer thicknesses. The first is a Si(2 nm)/Ge(1 nm)/Si(2 nm) superlattice where electrons can easily tunnel through the thin germanium 1 nm layer. The second is the Si(2 nm)/Ge(2 nm)/Si(2 nm) where tunneling is more likely for the

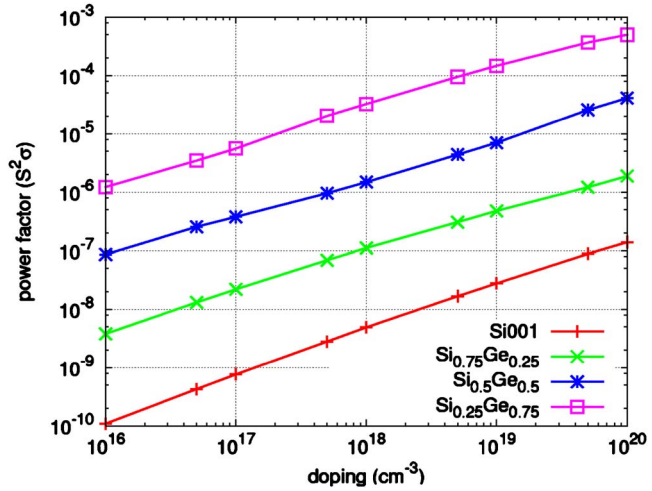

FIG. 7. (Color online) Power factor vs doping of Si(2 nm)/Ge(2 nm)/Si(2 nm) superlattice for various substrates.

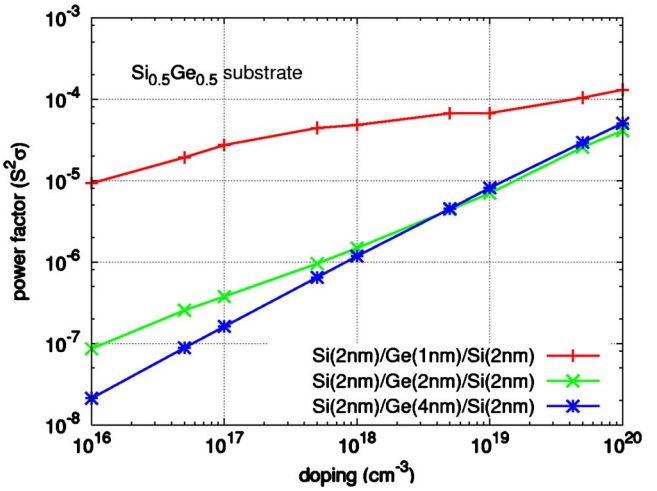

FIG. 9. (Color online) Power factor of Si/Ge/Si superlattices with $Si_{0.5}Ge_{0.5}$ substrate for varying thickness of the germanium layer.

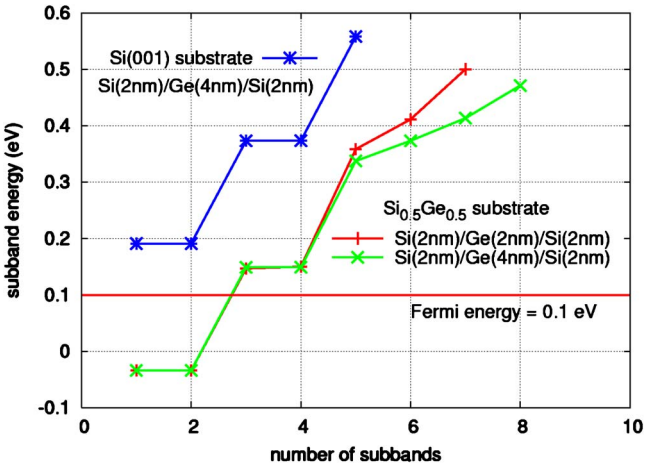

FIG. 10. (Color online) Comparison of subband energies of Si(2 nm)/Ge2 nm/Si(2 nm) and Si(2 nm)/Ge(4 nm)/Si(2 nm) superlattices on Si(001) and $Si_{0.5}Ge_{0.5}$ substrates.

superlattice on $Si_{0.5}Ge_{0.5}$ substrate compared to the Si (001) substrate for low doping. The third is a Si(2 nm)/Ge(4 nm)/Si(2 nm) superlattice where absolutely no tunneling is possible due to the very large germanium 4 nm barrier layer.

The electrical conductivity dominates the power factor for all cases considered with the superlattices grown on $Si_{0.5}Ge_{0.5}$ substrate, demonstrating higher power factors due to the lowering of silicon energy levels to below the Fermi level due to strain. For both substrates, the best power factor is obtained for the Ge 1 nm layer that allows electron tunneling through the superlattice, resulting in high electrical conductivity. For higher doping, the Si(2 nm)/Ge(2 nm)/Si(2 nm) superlattice has almost the same power factor as the Si(2 nm)/Ge(4 nm)/Si(2 nm) superlattice for $Si_{0.5}Ge_{0.5}$ substrate, as seen in Fig. 9. The reason for this behavior can be understood from Fig. 10 where the subband energies for superlattices with Ge (2 nm) and Ge (4 nm) have been plotted for $Si_{0.5}Ge_{0.5}$ and Si(001) substrates for a doping of 10^{19} cm^{-3}. For energy below the germanium barrier height, the subband energies in the superlattice occur in pairs. These levels originate from each of the two silicon wells in the three layer Si/Ge/Si superlattice. Since the subband energies correspond to the eigenvalues of the superlattice Hamiltonian, these subband energy levels are not the same as single silicon films having the same thickness as the well region. The actual current contributed by each of these subbands is determined by Green's function of the channel that takes into account the presence of the germanium barrier layer when calculating the channel density of states.

As seen from Fig. 10, the conduction band edge for the germanium layer with $Si_{0.5}Ge_{0.5}$ substrate lies below the Fermi level compared to the Si(001) substrate. As a result, the first few subband energies for a superlattice on $Si_{0.5}Ge_{0.5}$ substrate lie closer to the Fermi level compared to the Si(001) substrate, providing more states for electron transport. In addition, the 4 nm germanium layer also has more subband energies available for transport within a given energy range. This is evident from Fig. 10 where between the energy range of −0.1 and 0.5 eV, the superlattice with 4 nm Ge layer on $Si_{0.5}Ge_{0.5}$ substrate has one additional subband compared to the superlattice with 2 nm Ge layer on $Si_{0.5}Ge_{0.5}$ substrate.

The similar thermoelectric performance of the higher doped 2 and 4 nm Ge superlattices on Si_xGe_{1-x} substrates can be taken advantage of during the fabrication of superlattices where interdiffusion between very thin layers can be avoided by using a thicker germanium layer to obtain the desired thermoelectric performance.

III. CONCLUSIONS

Lattice strain induced from epitaxially grown materials with a lattice mismatch can have a significant impact on the thermoelectric performance of superlattice devices. Strained superlattice layers show higher power factors due to lowering of conduction band minima with strain. In the Si/Ge/Si device, results show that substrates rich in germanium will lower the energy of the conduction band valley in silicon sufficiently enough to provide more states around the Fermi energy for electron transport. Such substrates also produce oscillations in the Seebeck coefficient that are attributed to change in electron tunneling probability due to the shift in subband energies around the Fermi level with doping. These effects cannot be captured in semiclassical models without introducing some form of quantum corrections. The Seebeck oscillations produced by germanium-rich substrates could be exploited to design structures with high power factors for low doping. In addition, while large barriers block electron transport at low doping leading to poor power factors, substrate strain lowers the subband energies sufficiently enough that a 4 nm barrier layer demonstrates better thermoelectric performance than a 2 nm barrier. This fact can be exploited to design superlattice layers with large barriers that offer enhanced power factors so that problems with interlayer diffusion can be avoided.

ACKNOWLEDGMENTS

This material is based upon work supported by the National Science Foundation under Grant No. 0554089 and a Vanderbilt Discovery Grant.

[1]J. J. Welser, J. L. Hoyt, S. Takagi, and J. F. Gibbons, Tech. Dig. - Int. Electron Devices Meet. **1994**, 373.
[2]K. Rim, J. J. Welser, J. L. Hoyt, and J. F. Gibbons, Tech. Dig. - Int. Electron Devices Meet. **1995**, 517.
[3]K. Rim, J. L. Hoyt, and J. F. Gibbons, Tech. Dig. - Int. Electron Devices Meet. **1998**, 707.
[4]J. L. Hoyt, H. M. Nayfeh, S. Eguchi, I. Aberg, G. Xia, T. Drake, E. A. Fitzgerald, and D. A. Antoniadis, Tech. Dig. - Int. Electron Devices Meet. **2002**, 23.
[5]M. S. Dresselhaus, Y. M. Lin, T. Koga, S. B. Cronin, O. Rabin, M. R. Black, and G. Dresselhaus, in *Recent Trends in Thermoelectric Materials Research III*, Semiconductors and Semimetals Vol. 71, edited by T. M. Tritt (Academic, New York, 2001), Chap. 1.
[6]S. Takagi, J. L. Hoyt, J. J. Welser, and J. F. Gibbons, J. Appl. Phys. **80**, 1567 (1996).
[7]A. Balandin and K. L. Wang, Phys. Rev. B **58**, 1544 (1998).
[8]A. Balandin and K. L. Wang, J. Appl. Phys. **84**, 6149 (1998).
[9]L. D. Hicks, T. C. Harman, and M. S. Dresselhaus, Appl. Phys. Lett. **63**, 3230 (1993).
[10]L. D. Hicks and M. S. Dresselhaus, Phys. Rev. B **47**, 12 727 (1993).
[11]L. W. Whitlow and T. Hirano, J. Appl. Phys. **78**, 5460 (1995).
[12]B. Yang, W. L. Liu, J. L. Liu, K. L. Wang, and G. Chen, Appl. Phys. Lett.

81, 3588 (2002).
[13]D. Vashaee and A. Shakouri, J. Appl. Phys. **95**, 1233 (2004).
[14]S. Datta, *Quantum Transport: Atom to Transistor* (Cambridge University Press, New York, 2005).
[15]A. Bulusu and D. G. Walker, J. Heat Transfer **129**, 492 (2007).
[16]A. Bulusu and D. G. Walker, "Quantum modeling of thermoelectric properties of Si/Ge/Si superlattices," IEEE Trans. Electron Devices (to be published).
[17]C. G. Van de Walle, Phys. Rev. B **39**, 1871 (1989).
[18]R. Muller, T. Kamins, and M. Chan, *Device Electronics for Integrated Circuits* (Wiley, New York, 1986).
[19]B. Yang, J. Liu, K. Wang, and G. Chen, *2001 Materials Research Society Symposium Proceedings*, Vol. 691 (Materials Research Society, Pittsburgh, November 26-30, 2001), p. 71.
[20]B. Yang, J. L. Liu, K. L. Wang, and G. Chen, Appl. Phys. Lett. **80**, 1758 (2002).
[21]W. L. Liu, T. B. Tasciuc, J. L. Liu, K. Taka, K. L. Wang, M. S. Dresselhaus, and G. Chen, *Proceedings of the 20th International Conference on Thermoelectrics (ICT)*, June 8-11, 2001, pp. 340–343.
[22]T. Koga, S. B. Cronin, M. S. Dresselhaus, J. L. Liu, and K. L. Wang, Appl. Phys. Lett. **77**, 1490 (2000).
[23]D. Vashaee, Y. Zhang, A. Shakouri, G. Chen, and Y.-J. Chiu, Phys. Rev. B **74**, 195315 (2006).
[24]R. Venkatasubramanian, T. Colpitts, E. Watko, and D. Malta, Proceedings of the Spring Meeting of Materials Research Society, San Francisco, April 1997.